CrystEngComm

Accepted Manuscript

ROYAL SOCIETY OF CHEMISTRY

www.rsc.org/crystengcomm

CrystEngComm

RSCPublishing

HIGHLIGHT

Nanostructure formation via post growth of particles

Cite this: DOI: 10.1039/x0xx00000x

Bing Ni, Xun Wang*

Received 00th January 2012,
Accepted 00th January 2012

DOI: 10.1039/x0xx00000x

www.rsc.org/crystengcomm

Post growth of particles will lead to new nanostructure formation, and blur the boundaries of crystal growth and molecular chemistry, too. The driving force of post growth usually stems from the inherent stabilities of nanoparticles (NPs) and the environment changes, which results in the transformation of pristine nanostructures. One type of the post growth driven by thermodynamic stability is Ostwald ripening, which usually leads to the elimination of small particles, can be utilized to prepare hollow structures, too. By sophisticatedly controlling over reaction conditions, the NPs may undergo oriented attachment to form nanostructures with more complexity. This process is different with random aggregation of nanoparticles, the final morphologies can be ingeniously controlled, and the kinetics resembles polymerization in some cases. If the chemical bonding during oriented attachment process is replaced by non-covalent bonding, self-assembly of NPs is achieved. Self-assembling of NPs further extend the diversity of nanostructures, as well as the understanding of crystallization. Post growth of particles is also a feasible strategy to fabricate heterostructure. The wetting behaviour sheds light on the final morphologies of heterostructures. Meanwhile, seed mediated growth enables alternating method to control over pre-formed NPs. Another heterostructure of atomic-thin layered sheets connected via van der Waals force also extends the potential of nanomaterials. The driving forces of post growth of particles are divergent, and applications are various. They can be utilized to prepare homogeneous and heterogeneous structures.

1. Introduction

The classic crystal growth theory, especially the classic nucleation theory (CNT) is now facing challenge. Classic crystal growth theory is based on that crystal nuclei form from fluctuation of ion concentrations, then followed by atom-by-atom or monomer-by-monomer addition to form crystal. CNT has led to great success in materials synthesis[1], and can withstand the examination of atomic resolution imaging under certain conditions[2], however, it may not under other conditions[3]. The main challenges for classic crystal growth arose from mesocrystal formation and oriented attachment[4]. Biomineralization often involves mesocrystal formation, especially in the case of $CaCO_3$ formation[5-7]. Mesocrystal formation contradicts CNT, the contradiction may lie on the gap between thermodynamics and kinetics. Thermodynamic expression represents the statistic average of huge amount of particles at equilibrium state. However, the roles of rate are underestimated. Oriented attachment which would be seen as a kind of post growth of particles occurs in many cases, and is inconsistent with the atom-by-atom growth manner. In short, the details of crystal formation require further studies to unravel the whole process. Fortunately, with the help of advanced analytical techniques, we can directly observe the transformation of formed particles, thus review of post growth of formed particles could shed light on the big picture of crystal growth theory. Though many parts in this review have been individually reviewed in many papers, however, they are seldom organized together, in order to give a comprehensive study of post growth of nanocrystals and extend understanding of molecular and crystals.

The last several decades have witnessed the fast development of fabrications of nanomaterials. However, nanoparticles (NPs) are usually thermodynamically unstable comparing with their bulk states, especially when the protecting environment, like capping ligands and storing solution, changes. Thus post growth of NPs may take place. Herein the term “post growth” are related to structure change of formed particles.

Various nanostructures can be achieved via post growth of particles under certain conditions, albeit post growth may lead to aggregation of NPs in many cases.[8] In fact, the post growth of particles blurs the boundary of behaviours of crystals and molecules. Reactions and polymerizations of NPs may follow the rules of molecular chemistry. Such observations would greatly extend our view of chemistry. For convenient, we divide this review chiefly into two parts, based on homogeneous or heterogeneous structures, though some examples cross the line between them. Post growth of homogeneous structure implies the inherent properties of NPs, thus we begin gradually from their thermodynamic stabilities to Ostwald ripening, oriented attachment. Then we further extend the scope of growth, self-assembling of NPs is seen as another growth which doesn't involve the formation of new chemical bonds, instead, other driving forces are required. Process that second compound reacts with the already formed NPs is seen as the post growth to form heterostructures, albeit not all final products are real heterostructures constituted by various compounds because of the elimination of one compounds. We start with the

conventional wetting process to illustrate the possible final morphologies, then particle fusion is described. If the second nanomaterial is fabricated by utilizing pre-formed seeds, we consider this as seed mediated growth. Seed mediated growth enables new synthetic strategies for NPs, based on the properties of pre-formed NPs. Van der Waals heterostructures developed from various atomic-thin layered materials are promising for electronic device, and we also briefly introduce them.

2. Post growth of homogeneous structure

2.1 Thermodynamic of nanoparticle

The formation of NP is complicated, which usually involves chemical reactions of precursors, adsorption of ligands, growth of crystal, etc. In general, NPs experience various stages from metal precursor, to nuclei, then crystal seeds and finally enlarge to form the available particles.[9] The rationale of nanomaterials lies on thermodynamic or kinetic stabilities under reactions. Thermodynamics which only concern the initial and final states of the system, is a powerful tool to analyse the stability of NPs, albeit the details of formation may be unknown.

Taking a spherical NP as an example, the Gibbs free energy of formation can be expressed as the sum of volume energy and the surface energy change:

$$\Delta G_{tot} = \Delta G_{vol} + \Delta G_{sur} = \frac{4}{3}\pi r^3 G_v + 4\pi r^2 \gamma_u \qquad \text{equ(1)}$$

Here ΔG_{tot} is the total energy change from initial state to final state, ΔG_{vol} is the volume energy change and ΔG_{sur} denotes the energy change on surface, r is the radius of sphere, G_v is the energy per unit volume, γ_u is the surface energy per unit area of surface. The particle forms a new phase which doesn't exist in initial state, so G_v and γ_u are not in form of Δ. The energy change can be divided into two parts: volume energy change and surface energy change, the equation in left depicts a general rule of NP fabrication. The crystal structure of products determine G_v, so this term could not be changed when the compound has chosen. However, the surface energy could alter with morphologies. The surface energies of different facets usually increase in the order $\gamma(111) < \gamma(100) < \gamma(110)$.[10] In an ideal situation, a polyhedron with sharp edges would be preferred only with (111) facets. However, this is not always the case in real NP preparation, because the surfactant or capping agent in the synthesis may preferentially bind on certain facets and change their surface energies. On the other extreme, a spherical shape is more feasible when all of the facets of a nanocrystal are equally favoured. Because the spherical shape possesses lowest surface atoms when compared with other shapes of same volume, thus the surface energy is the lowest in this case. The spherical shape is always adopted in amorphous solid. In fact, most NPs lie in between these two extremes.[11]

When the NP reaches thermodynamically stable shape, the surface free energy must be minimum for a given volume.[12] Wulff construction is aimed to reconcile the surface energies with certain volume. The surface energies of any particles could be written in the form:

$$\Delta G_{sur} = \int \gamma(n) dS \qquad \text{equ(2)}$$

Here γ is the specific surface free energy of orientation that the unit outward normal n at each surface point. Solid line in Figure 1 depicts γ as a function of n in a two-dimensional cross section

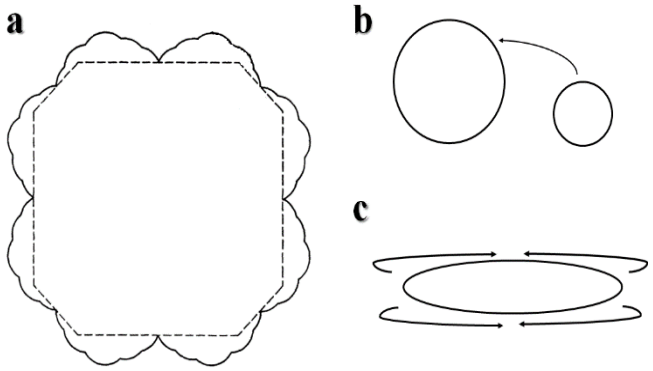

Figure 1 Scheme of Wulff construction (a), inter-particle (b) and intra-particles (c) Ostwald ripening. Solid line depicts surface energy in a two-dimensional cross section of crystal, and the stable morphology would be like the shape drawn as dash line. The arrows in (b, c) illustrate the mass transfer from one area to another, in order to decrease curvatures, as well as energies.

of crystal. The final shape of NP would be similar with the shape drawn by the dash line, according to Wulff construction. Since thermodynamics cannot explain every phenomena, kinetic effect must be concerned for real situations[13].

Though thermodynamics fails in detailing the growth mechanism, the prediction of NP's stability could also help to well-design the morphology. When NP doesn't reach the most stable shape, thermodynamic would drive the post growth of NP. Even the NP achieves a stable structure, the post growth of NP may also happen because of the change of environment.

2.2 Ostwald ripening

The birth of NP is a competition of chemical reaction, atom diffusion, particle growth, dissolution, etc. Lots of parameters of reaction would affect the shape and size of final products. Thus the size of NPs cannot be exactly the same even in the same batch. No matter how uniform the products are in characterization, the sizes must distribute in a range. However, the surface energy of single particle depends on the curvature, and this would be the driving force for post growth of NPs with inappropriate size:[14]

$$\mu = \mu_0 + V_m \gamma \kappa \qquad \text{equ(3)}$$

Here μ and μ_0 are chemical potential of curving and flat interface, V_m is the molar volume, γ is the surface energy and κ is the mean interfacial curvature. Thus we know that the stabilities of NPs of different sizes are different. "The total energy of the two-phase system can be decreased via an increase in the size scale of the second phase and thus a decrease in total interfacial area", this is called Ostwald ripening.[14] From equ(3), we can know that the atoms will flow from regions of high to low curvature, this results in vanishing of small particles and further enlargement large particles (Figure 1b). The final distribution is independent with initial environments but relies on final environment.[15]

Ostwald ripening would be detrimental in some cases. The luminescence properties of semiconductor NPs are related to their sizes. However, due to the Ostwald ripening, CdS quantum dots grows larger, shifting their spectrum.[16] This is also true in other II-VI semiconductors. Individual fractions of CdTe, CdSe or InAs separated from the same batch synthesis by size-selective

precipitation could have different photo luminescence quantum efficiencies.[17] Ostwald ripening could happen not only at inter-particle, but also at intra-particles. In CdSe NP fabrication, the process is controlled by the monomer concentrations.[18] At high monomer concentrations, rod shape NPs would grow, while at low concentrations, the aspect ratio depends on the intraparticle diffusion on the surface of different facets, driven by surface energy differences (Figure 1c).

Ostwald ripening drives smaller particles to dissolve and larger particles to growth, usually the size distribution grows larger and larger. However, this kind of dissolution and regrowth method could be utilized to prepare uniform NPs with narrow size distribution, too. Ostwald ripening of the hexagonal β-phase of $NaREF_4$ (RE: Sm, Eu, Gd, Tb), would lead to the expected growth broaden particle size distributions, and $NaLaF_4$ would decompose to LaF_3. However, Ostwald ripening of α-phase would result in two possible endings: one is β-phase product with larger size but very narrow size distribution and other is smaller particles of the rare earth trifluoride REF_3. These two different scenarios of Ostwald ripening arose from stabilities and dissolving rate of different phases.[19]

The driving force of dissolution and regrowth could be extended from Ostwald ripening to other situations, like chemical etching, thus NPs with high quality could be generated. Noble metal NPs with high yield and uniformity could be achieved by iterative reductive growth and oxidative dissolution reactions.[20] The dissolution and regrowth method is a powerful tool to accomplish high quality NPs or other materials like graphene[21].

Ostwald ripening process of NPs could also help to fabricate new morphologies. Ag nanosheets, chainlike sheets and microwires could be easily generated via an ammonia-assist Ostwald ripening mechanism.[22] Ostwald ripening of $ZnIn_2S_4$ nanosheets would result in a spherical shape.[23] Surface clean structure could easily undergo Ostwald ripening because of the lack of protection ligand on the surface. Electrochemically deposited Ag nanoplate-assembled micro-hemisphere structure can change to well aligned nanoplates at suitable condition.[24] Aggregation of vast small spheres can construct a big sphere,

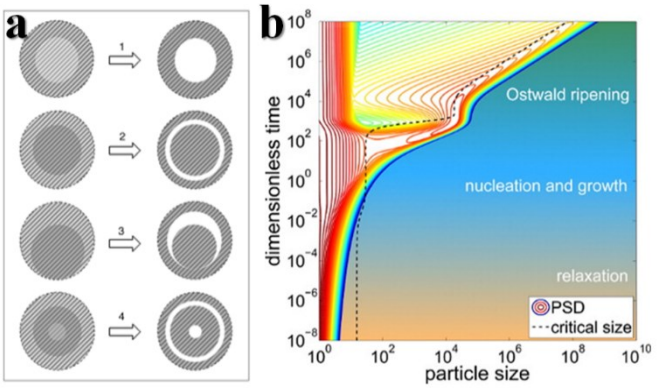

Figure 2 (a) Various schemes of Ostwald ripening for spherical colloidal aggregates: 1) core hollowing process; 2) formation of a homogeneous yolk-shell structure; 3) formation of a semi-hollow yolk-shell structure; 4) combination of 1 and 2. The shadow denotes small spherical particles. In the process, unstable spheres are vanished. Reproduced with permission from ref. 26. Copyright 2005 WILEY-VCH Verlag GmbH & Co. KGaA, Weinheim. (b) Modelling nucleation, growth and Ostwald ripening in crystallization processes. Red color indicate uniform size. Reproduced with permission from ref. 30. Copyright 2013 American Chemical Society (ACS).

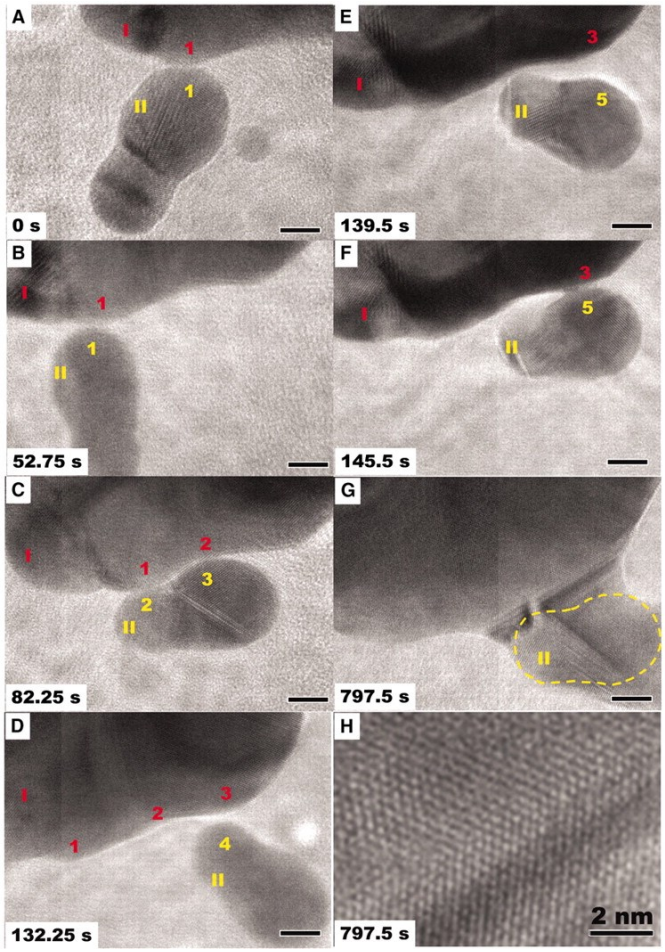

Figure 3 (A to G) Sequence of images showing typical dynamics of the oriented attachment process. The surfaces of particles I and II made transient contact at many points and orientations (points 1-1, 1-2, 2-3, and 3-4) before finally attaching and growing together (points 3-5). (H) High-resolution image of interface in (G) showing twin structure (an inclined twin plane). Reproduced with permission from ref. 39. Copyright 2012 American Association for the Advancement of Science (AAAS).

however, the stabilities of the spheres in big sphere are different, after ripening, the most stable spheres stay. This strategy could help to synthesize hollow structure (Figure 2a). TiO_2 hollow sphere[25], ZnS and Co_3O_4 yolk-shell structure[26] can be fabricated via etching the less stable nanospheres inside the aggregations with the help of ions remained in the synthesis of sphere. The process is similar with Kirkendall effect[27], which illustrates the preparation of hollow structures using the differences in diffusion rates of various component via introducing etchant. However, their driving forces are quite different. When we consider atom transfer at multicomponent NPs, the movement of different kinds of atoms inside will lead to hollow structures.[28, 29]

Crystal nucleation, growth, and Ostwald ripening could be reconciled theoretically via a model based on the kinetic rate equation (Figure 2b).[30] The transition between ripening and growth is caused by the relationship of particle size and particle size distribution (PSD), as well as the dimension time. Real-time *in situ* high-resolution electron micrographs reveal that crystal shrinkage and growth may take place at the same time during

Ostwald ripening, and the shrinkage proceed possesses lower activation energy barrier compared to growth.[31]

2.3 Oriented attachment

Ostwald ripening reveals the instability and transformation of NPs. However, the unstable NPs may not just disappear, anisotropic NPs may attach together to form larger particles in order to decrease the surface energy. Such kind of growth mechanism is based on the post growth of particles rather than classic crystal growth theory. There is a themed issue of oriented attachment on *CrystEngComm*[32], both comprehensive[33-36] and specific[37, 38] papers are there. Oriented attachment is common in fabrication of nanomaterials, here we briefly introduce oriented attachment to get a comprehensive review on post growth of particles.

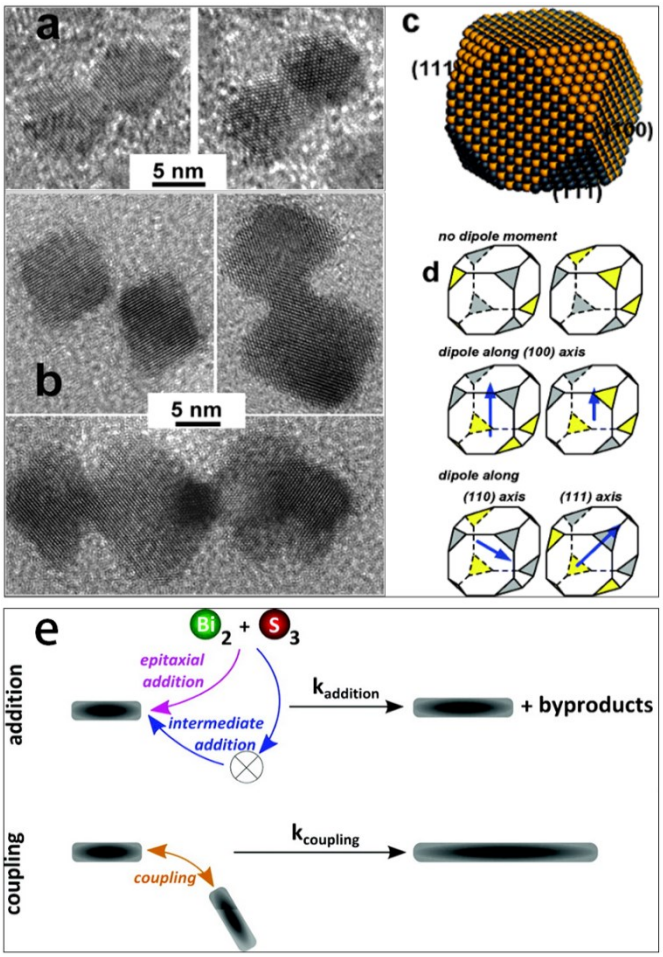

Figure 4 High-resolution TEM images showing oriented attachment of PbSe nanocrystals. (a) Two nanocrystals attached along the <100> crystallographic direction viewed along the (100) and (110) zone axes. (b) Attachment of PbSe nanocrystals along the <110> crystallographic direction (viewed along the (100) zone axis). (c) Atomic reconstruction of a rocksalt PbSe nanocrystal showing the structural difference between the [100] and [111] facets. (d) Different arrangements of polar [111] facets result in various orientations and magnitudes of the nanocrystal dipole moment. Yellow and gray color indicate Se termination of [111] and [110] respectively. Reproduced with permission from ref. 41. Copyright 2005 ACS. (e) Diagram illustrating the two steps used to describe the growth mechanism of the Bi2S3 nanowires. The addition step involves the addition of molecular precursors or intermediates (clusters or complexes) to the tips of the nanowires. This molecular process is expected to produce one or more condensation byproducts. The coupling step involves the attachment of two nanowires by their tips. Reproduced with permission from ref. 42. Copyright 2010 ACS.

The inherent properties could drive the oriented attachment of NPs. *In situ* high resolution transmission electron microscopy can track the whole process of the oriented attachment of iron oxyhydroxide NPs in detail (Figure 3). Two particles adjust their positions in order to find a perfect lattice match, then a sudden jump to contact take place, followed by interface elimination to fully fusion.[39] The driving force of oriented attachment is similar to Ostwald repining, the high energy surface tends to vanish by attachment instead of elimination of whole NPs. The transformation could be triggered by the introduction of competing ligands.[40] Meanwhile, the attachment of NPs may also require proper interactions between single NPs. Taking the attachment of PdSe as an example[41], the dipole moment between NPs is vital for the attachment manner. The small PbSe NPs are encapsulated by six [100] facets and eight [111] facets, their polarities are different due to the difference in electronegativities between Pb and Se and their termination manner (Figure 4c, d). Single NPs can either have central symmetry and thus show a zero net dipole moment or they can lack central symmetry and show certain dipole moment, depending on the atom arrangement of [111] facets. By controlling the morphologies of NPs and the reaction conditions, various oriented attachment structure can be achieved (Figure 4a, b).

Is the attachment process quite similar to polymerization? The answer is yes in some cases. When taking a closer look at the kinetics of attachment of Bi_2S_3, the process resembles living step-growth polymerization[42]. There are two possible mechanisms to prepare the ultrathin Bi_2S_3 nanowires (Figure 4e). One is addition method, monomers of Bi ions and S ions directly or indirectly grow on the end of nanorods and elongate the rods to long wires. The details of addition are not clear, however, the kinetic data could be calculated by using mathematics same with polymerization. The other method is growth via coupling, i.e. attachment of different rods to form long nanowires. The diameter of rods and wires remains constant during the synthesis, this is a good strategy to prepare long nanowire with uniform diameters. Meanwhile, the study demonstrates a physical analogy between crystallization and polymerization. A recent research in our group also find similarities between the formation of inorganic single wall nanotube and radical polymerizations (manuscript in preparation).

Oriented attachment opens new way for material design, more and more findings prove the similarities between crystallization and polymerization. All the findings enlighten us to view the post growth of particles in a new sights. So what if that particles don't attach and reconstruct to a new crystalline structure? This is actually a common phenomenon in nanoscience called self-assembling.

2.4 Crystal and self-assembling

The second law illustrates that isolated system prefers disorder. However, from lab to society, life to work, people are fond of order. Crystal is a bunch of atoms arranged in specific manner. The versatile properties of crystal stems from the element composition and stacking styles. What about the

specifically arranged crystal? Band of photon, which resembles energy band of crystal, could be generated in an ordered assembling structure when the distance between crystals is comparable with light wavelength[43]. The self-assembling of nanocrystals shares some features with crystal, such as the rules of growth in some situations. The generation of self-assembling could be achieved via the post growth of NPs, while single NPs usually maintain their original characters.

Another important reason that we need to pay attention to self-assembling is that it's very interesting. "Specifically arranged crystal" is not a scientific expression, for it doesn't explicitly specify a specific field. Thus any NPs could generate self-assembling structures. This would greatly extend the research scope. In addition, the driving forces of assembling are divergent, such as van der Waals forces, electrostatic forces, magnetic interactions, etc.[44], this further expand the scopes. The scale of self-assembling could bridge the gap between micro to macro, which make the nanosized particles a practical materials. Well-designed assembly resembles hierarchical structure of bio-molecules, which we could utilize to construct functional materials in multi-scale, the size in larger scale enables us to manipulate the structure by conventional lithography method.[45, 46] Yet more self-assemblies would dramatically increase our understanding about chemistry. Supramolecule chemistry deals with world beyond molecule[47], while self-assembling of crystals may be more complicated because they deal with interactions beyond a bunch of crystals.

The direct consequence of ordering is that the decrease of entropy.[48] Entropy, together with spherical confinement, could make numerous spheres to form icosahedral clusters.[49] This research sheds light on the formation of icosahedral symmetry, tens of thousands of spheres compressed under spherical would spontaneously form icosahedral clusters, because they are entropically favoured comparing with the bulk face-centred cubic crystal structure[50]. However, directly determining the precise entropy change could be difficult[51], and may be unworthy for the weakness in intuitional transition to other systems to guide fabrications, albeit sights from entropy may touch the nature of self-assembling. Thus describing the formation of self-assembling from the sights of force would be more convenient and intuitional.

Spiral assembling structure is one of the most intriguing assemblies, there are several very different method to achieve it. Magnetite nanocubes can assemble into helical superstructures in the presence of magnetic field under carefully controlled conditions (Figure 5A-F).[52] Detailed studies revealed that NPs with different anisotropic structures, i.e. truncated octahedra, rounded cubes, cube-sphere heterodimeric NPs, behave differently under the same condition, suggesting the interplay of NPs with external magnetic field would determine the final helical assembling structure. Chiral structures are interesting and common in nature, however the origin of chirality stays in fancy. Circularly polarized light (CPL) may serve as chiral tempting for self-assembly. Right- (left-)handed CPL could convert CdTe NPs to form right- (left-)handed twisted nanoribbons with an enantiomeric excess of more than 30%, which is about 10 times higher than that of conventional CPL-induced reactions.[53] Light can induce the conversion of thioglycolic acid protect CdTe NPs to CdS NPs, the effect of CPL induced transformation lies on the optically selective activation of nanostructure with different handedness. The process requires deeper study in order to yield enantiopure materials in a more efficient way.[54] Stirring may induce the formation of chiral assembly, too. With the help of Pluronic P123, an achiral triblock copolymer, several one-

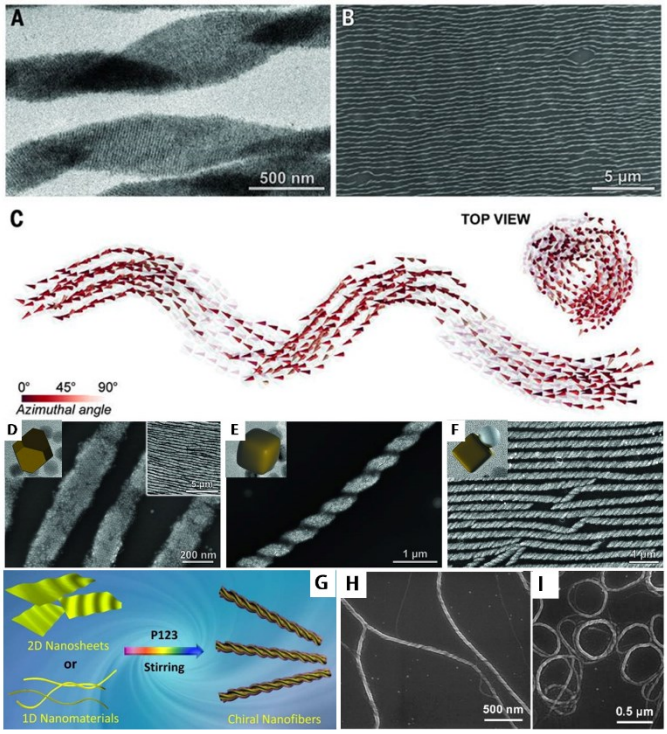

Figure 5 Self-assembly of helical nanocrystal superstructures. (A, B) TEM image of individual single-stranded helices constituted by Fe3O4 nanocrystals under magnetic field. (C) Snapshots from Monte Carlo simulations of a one-dimensional belt folding into a helix. Self-assembly of Fe_3O_4 nanocrystals of different shapes: truncated octahedral (D), rounded cubes (E), and Fe_3O_4-Ag heterodimer (F). Reproduced with permission from ref. 52. Copyright 2014 AAAS. (G) Stirring in the present of P123 could lead to chiral structure formation from one or two dimensional ultrathin materials. (H, I) depict the chiral structures of graphene oxides caused by stirring. Reproduced with permission from ref. 55. Copyright 2015 ACS.

dimensional and two-dimensional ultrathin nanomaterials can self-assemble into chiral structure under vigorous stir (Figure 5G-I).[55] Helical and chiral structure remains intriguing for material synthesis, especially for the construction from achiral ordinary structure. Unrevealing the mystery beneath formation of chirality may help us to better understand the origin of life molecules.

Modifying the surface of NPs could enable more versatile assemblies. Au NPs coated with dextran enable linear self-assembly[56], and Au NPs coated with pH-responsive polymer brushes can reversibly construct into linear chains by stepwise tuning of the environmental pH value.[57] The linear chains are quite similar with block polymers, by considering single Au NP as block chain. Could the assembling kinetics resemble the polymerization of unsaturated molecules? The answer is yes, but ingenious design is required. Anisotropically coating a bilayer of cetyltrimethyl ammonium bromide along its sides and thiol-terminated polystyrene on the head of Au nanorods, could enable step growth polymerization of Au nanorods, stemming from the difference of interactions between sides and heads and similarity of interactions between heads to heads.[58] The growth kinetics is similar to step growth polymerization of polymers. The interaction between two NPs could also extend to metal

coordination.[59] With the help of capping the ends of NPs with specific surfactant of available ligand, the assembling manner can be well-controlled by utilizing the specific affinity between ligand and additive metal ions. The strategy could extend to smaller scale. Molecule cages with or without cluster encapsulated can assemble to intricate structures.[60] More and

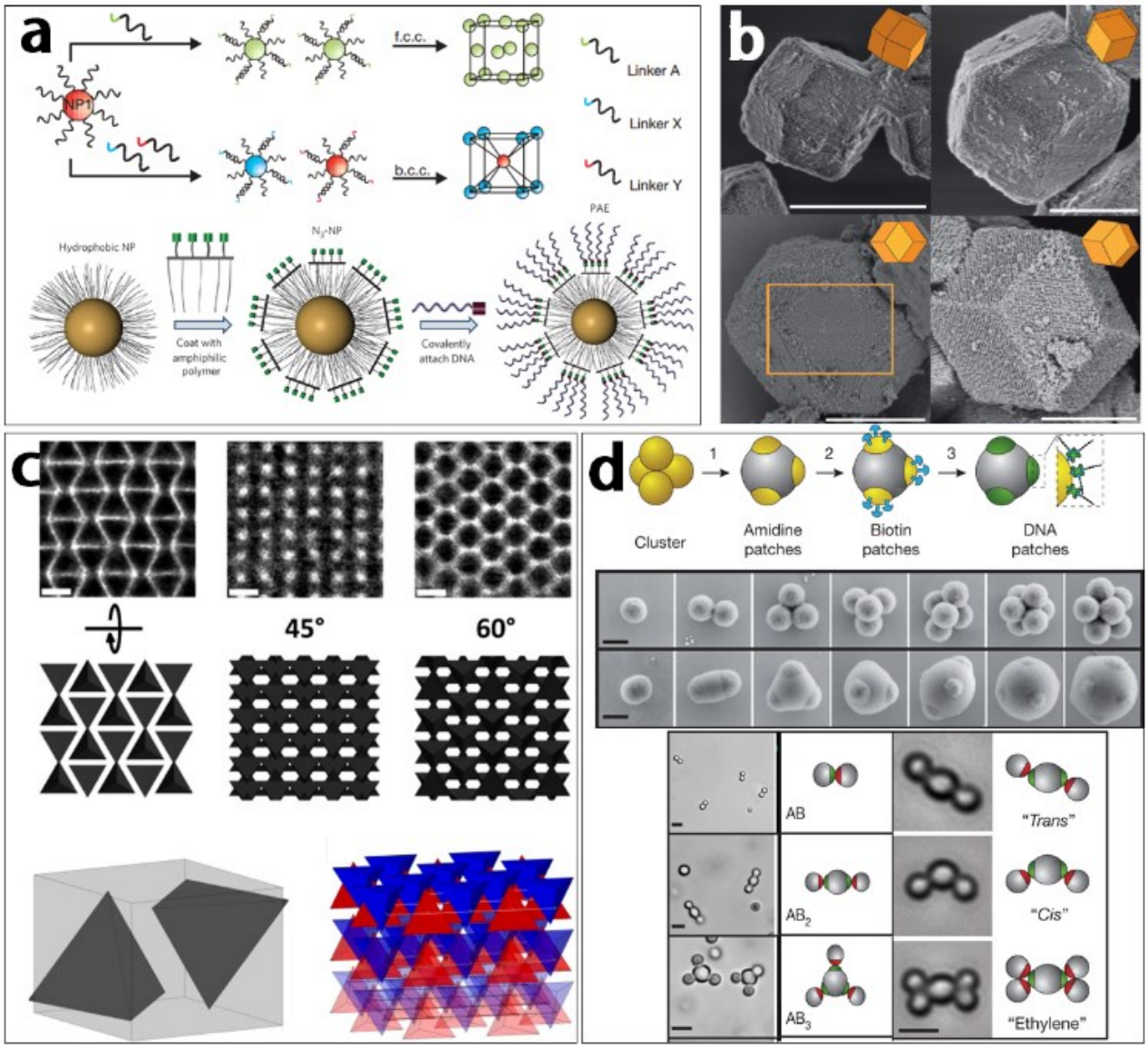

Figure 6 (a) NP–DNA conjugates can be assembled into different crystallographic arrangements by changing the sequence of the DNA linkers. To further extend the possibility of DNA assist self-assembly, a general method is required. Hydrophobic-ligand-capped nanoparticles were first functionalized with an amphiphilic polymer containing both hydrophobic alkyl chains (which intercalated with the hydrophobic capping ligands on the nanoparticle, shown as grey brushes) and hydrophilic carboxylates and azide- (green) modified ethylene glycol groups that solubilized the particles in aqueous solvent. These particles were then functionalized with DNA using dibenzocyclooctyl- (purple) terminated DNA strands and azide–alkyne click chemistry to produce a dense DNA shell around the nanoparticle. Reproduced with permission from ref. 62, 64. Copyright 2008, 2013 Nature Publish Group (NPG). (b) The morphology of assembly of Au particles may suit the Wulff construction, here shows a rhombic dodecahedron microcrystals viewed from various orientations. Reproduced with permission from ref. 67. Copyright 2014 NPG. (c) Assembly of loose structure constituted by tetrahedron viewed from various orientations, cartoons below shows the packing manner. Reproduced with permission from ref. 68. Copyright 2014 ACS. (d) Self-assembling structure could also mimic the behaviour of covalent bond. A four-patch particle is shown as an example. 1, a cluster of four amidinated polystyrene microspheres is swollen with styrene such that the extremities of the cluster—a tetrahedron in this case—protrude from the styrene droplet. The styrene is then polymerized and the protrusions from the original cluster become patches. 2, biotin is site-specifically functionalized on the patches. 3, biotinated DNA oligomers are introduced and bind to the particle patches via a biotin–streptavidin–biotin linkage. The as-prepared patchy particles could stick together in the way like organic molecules. Reproduced with permission from ref. 59. Copyright 2012 NPG.

more findings support that there is no rigid boundary between different fields of chemistries, all knowledge of chemistry may play special roles in various studies.

Yet chemists can control the polymerization process and make the polymers irreplaceable in society, could we enable programmable self-assembling? Programmable self-assembling not only demonstrates the power of chemistry, but also brings possibilities of new and efficient method to code information.[61] Among all the methods of programmable self-assembling, DNA assist assembling has shown power on controlled assembly, and it's the most promising method for conventional control the structure of assembly. The programmability of DNA assist self-assembly originates from that different DNA sequences could steer the same type of Au NPs to different crystalline states, such as face-centred-cubic or body-centred-cubic assembling structures (Figure 6a).[62] Anisotropic NPs could be used to construct anisotropic structure through anisotropic interactions resulting from particle shape or face-selective functionalization.[63] By utilizing DNA modifying, one-, two-, and three-dimensional structures that are impossible to realise via spherical particles. So far, we have discussed about DNA functionalization directly on the NP surface, however, not all NPs could be easily get in-contact with DNA, thus a variable strategy is required. NPs are usually fabricated in the present of hydrophobic ligands to prevent from aggregation, thus a transition ligand with azide group can deposit on the NPs due to the hydrophobic interaction, then DNA can attach with the NPs via copper-free azide-alkyne click chemistry. The modified NPs can self-assemble into various structures (Figure 6a).[64] The DNA assist assembly enables highly controlled and desired structure. For example, controlled-arranged Au nanorods achieved by DNA assistance shows novel optical properties[65] and encourage the development of nanophotonics.

The boundary between molecule chemistry and crystal assemblies might be further blurred. C atom which has four valence electrons is the soul of organic chemistry because of the divergent configurations. Meanwhile, NPs could also resemble the bonds of C. An assembling structure encapsulated with a second compound enable the anisotropic exposure of protrudent functional groups. Directional bonds can be formed along the protrudent parts (Figure 6d).[59] Au nanospheres could also assemble into anisotropic structures which imitate hybridized atomic orbitals of C, based on the energy transfer of assembling.[66]

The self-assembly shares feature with crystalline structures, not only in the packing manner of units, but also in the final morphologies of total structure. Wulff construction which is used to illustrate the stable morphology of NPs or crystals, can also help to explain the appearance of self-assembling structures (Figure 6b).[67] However, there are more possibilities of stacking in the assemblies, the reasons may be that the morphologies of stacking units differ from sphere to any shapes, meanwhile the free energy change is mainly caused by the entropy change in assembly, rather than enthalpy, which is also an inevitable parts for NP formation, thus structure with loose packing would likely be possible for assembly. Tetrahedral CdSe NPs could assemble into an open structure with spacing-filling fraction about 0.59, the loose packing may result from strong dependence of ligand-ligand interaction potential on NP surface curvature (Figure 6c).[68] Notwithstanding the packing density is related with the morphology of NP, the binary stacking of nanospherical particles are similar with crystalline salts (Figure 7).[69] More complicate multicomponent structures with the insertion of a third NP component at predetermined sites expand the scope of self-assembly.[70]

What about further decrease the size of building unit? Crystal

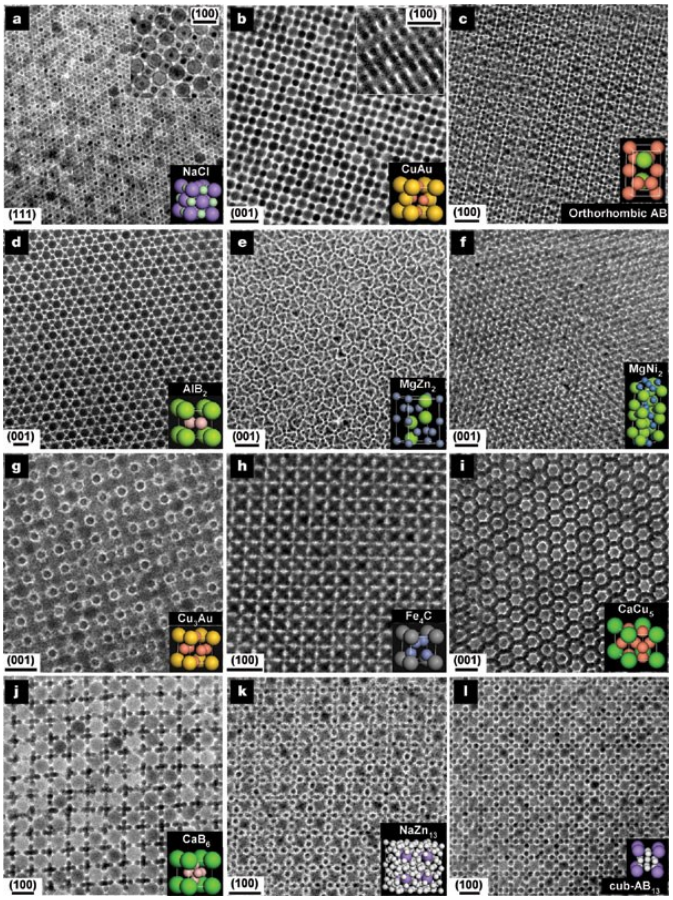

Figure 7 The superlattices are assembled from **a**, 13.4 nm - Fe_2O_3 and 5.0 nm Au; **b**, 7.6 nm PbSe and 5.0 nm Au; **c**, 6.2 nm PbSe and 3.0 nm Pd;**d**, 6.7 nm PbS and 3.0 nm Pd; **e**, 6.2 nm PbSe and 3.0 nm Pd; **f**, 5.8 nm PbSe and 3.0 nm Pd; **g**, 7.2 nm PbSe and 4.2 nm Ag; **h**, 6.2 nm PbSe and 3.0 nm Pd; **i**, 7.2 nm PbSe and 5.0 nm Au; **j**, 5.8 nm PbSe and 3.0 nm Pd; **k**, 7.2 nm PbSe and 4.2 nm Ag; and **l**, 6.2 nm PbSe and 3.0 nm Pd nanoparticles. Scale bars: **a**–**c**, **e**, **f**, **i**–**l**, 20 nm; **d**, **g**, **h**, 10 nm. The lattice projection is labelled in each panel above the scale bar. Reproduced with permission from ref. 69. Copyright 2006 NPG.

is built by the arrangement of atoms, what about clusters? Ultrasmall units open new gate for self-assembling.[71, 72] Using clusters to build assembly is a challenge, but not impossible. $[Co_6Se_8(PEt_3)_6][C_{60}]_2$, $[Cr_6Te_8(PEt_3)_6][C_{60}]_2$ are successfully achieved and they possess structure like CdI_2. $Ni_9Te_6(PEt_3)_8$ could transfer more charge to the fullerene and form a rock-salts-related structure[73], they undergo a ferromagnetic phase transition at low temperatures[74]. The properties of such materials need to be more explored since they extend our understanding of atoms.[75]

3. Post growth to form heterogeneous structure

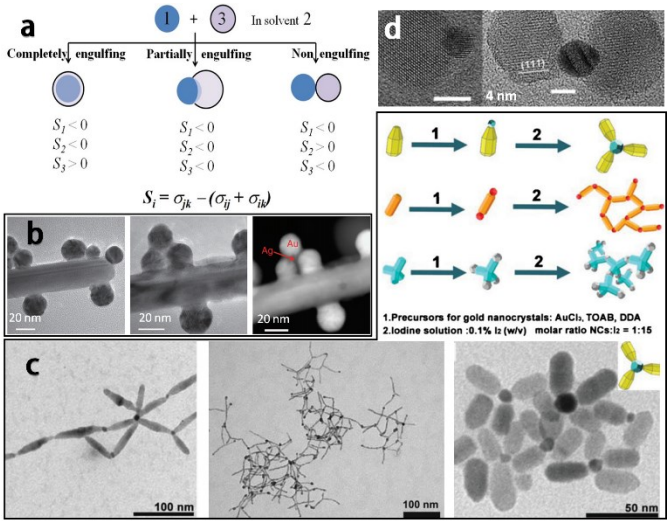

Figure 8 (a) Equilibrium configurations for two immiscible liquid droplets 1 and 3 in solvent 2, details are explained in text. Reproduced with permission from ref. 76. Copyright 2013 ACS. (b) Bright-field TEM and high-angle annular dark-field STEM images of gold NPs contacting a silver NR. It is clearly seen that the gold NPs do not change, whereas the silver NR 'climbs' to wet the gold spheres. Reproduced with permission from ref. 77. Copyright 2014 NPG. (c) Deposing Au dots at the end of rods could help to weld them, the welding shape could be tailored via the control over rods. The cartoons at upside depict fabrication and fusion manner of the images at downside. Reproduced with permission from ref. 80. Copyright 2009 WILEY-VCH Verlag GmbH & Co. KGaA, Weinheim. (d) two peanut-like particles could fuse together to generate dumbbell-like particles via linking by Au dots. Reproduced with permission from ref. 79. Copyright 2006 ACS.

3.1 Wetting

Wetting is very common seeing in nature, the rules of wetting are mainly used for cleaning. In general, wetting are usually controlled by the interfacial energies, which are termed to quantify the energy effect between the interfaces of different compounds. When combining two phases (1 and 3) in medium 2 (all of them cannot dissolve in each other phases, Figure 8a), three interfacial energies can be defined, σ_{12}, σ_{23} and σ_{13} (all are positive, phase 1 is selected such that $\sigma_{12} > \sigma_{23}$. The encapsulated behaviours depend on the relative value of these three interfacial energies $S_i = \sigma_{jk} - (\sigma_{ij} + \sigma_{ik})$, which is called spreading coefficients. For example, if phase 2 is "bad" solvent for phase 1 while "ok" solvent for phase 3, then it would be more favourable that phase 1 could hide in phase 2.

This is a simplified analysis based on geometric considerations. However, such simple rules may extend to analysis the post growth of second compounds on already formed NPs that whether they could form core-shell structure or other morphologies. The interfacial energies are proportional to the interfacial area, thus there are many parameters that could be tuned to optimize the structures. Meanwhile, they can also be qualitatively adjusted by lattice mismatch, the hydrophilicity / hydrophobicity of the surface ligands and the ligand density.[76]

3.2 Particle fusion

The wetting of Ag on Au can take place even on room temperature rapidly.[77] The wetting-driven merging phenomena render the large Ag nanorod wetting on small Au nanospheres (Figure 8b), which is intuitionally in contradiction with Ostwald ripening which smaller particles vanish. This is a typical case that wetting on nanoscale achieves the mobile of atoms. While in other cases, wetting drives the particles fuse together to form heterostructures. This phenomenon that several particles fuse is different with oriented attachment which large amount of NPs aligned and attached. If oriented attachment could be seen as the polymerization of NPs, then particle fusion which incorporates several NPs would be considered as reaction between NPs. This is a quite interesting analogy, such presumption may encourage us to research with new sights. Chemistry based on molecules and crystals enables plentiful new materials, thus particle fusion might bring new method for material design. On the other hand, linking nucleus-bridges between the closest faces of neighbouring crystals results in intergrowth of crystals[8], the process contains deeper insights of crystal growth.

There are several more examples of particle fusion to form new structures. The NPs fusion between CdS and ZnSe not only permit tuning of their emission spectra but also optimize the excited state lifetimes.[78] The fusion process is achieved simply via redispersing pre-synthesized ZnSe and CdS prolate nanodots in octadecene, while reaction annealing time could control the extent of the interfaces. "Soft" material served as "welding" is able to help the fusion of NPs. Au nanodots are usually used as "welding" to joint various nanomaterials, because Au can serve as seeds to fabricate different NPs and also deposit on diverse NPs, meanwhile Au nanodots could be active under certain etchants (Figure 8c). Seed mediated growth of Fe_3O_4, PbS or PbSe on Au nanodots would result in the formation of peanut-like NPs. The Au parts in two peanut-like particles could fuse together to generate dumbbell-like particles by adding sulphur into the system (Figure 8d).[79] Selective growth of Au tips on semiconductor nanorod, like CdS, CdSe or CdTe is available, then nanorods could link end-to-end with the help of I_2 which destabilize the Au tips and induce the coalescence if Au domains (Figure 8c).[80] Several different shapes are possible with the design of heterogeneous nanorods, and such metal-semiconductor nanocrystal forms a Schottky barrier.[81]

3.3 Seed mediated growth

Why do we need a seed mediated method to grow nanomaterials? The first reason is that heterostructures can be achieved via a deposition of new compound on the already formed seeds, meanwhile the seeds could guide the deposition manner. Usually the heterostructures show very different properties comparing with each of the single compounds.[82] Thus a seed mediated growth enables the fine optimization of properties. The second reason lies on that the seeds could serve as template to fabricate new homogeneous structures, such as galvanic etching, ion exchange, or sever as heterogeneous nuclei to grow heterostructures. Looking beyond this, NP seeds may play as the catalyst for material deposition, an extreme example is that vapour-liquid-solid and solution-liquid-solid method to fabricate nanowires[83]. Last but not least, the pre-prepared seeds could be utilized to generate unstable materials due to kinetic control. The seed mediated growth could help to synthesis large amount of new materials[84].

There exist many core-shell structures in the development of nanomaterial fabrications, here we take semiconductor NPs as an

example to illustrate the post growth of seeds to achieve core-shell structures. The motivations of preparation of core-shell semiconductor NPs are trying to improve photoluminescence quantum yield and achieve new properties comparing with both the core and shell materials. To accomplish that, the size of core is tailored to be uniform and stable under post grow, meanwhile the shell material only grows on core seeds.[85] In order to supress the homogenous nucleation of separate shell materials, several methods has been proved accessible. Successive ion layer adsorption and reaction (SILAR) which is similar with atomic layer deposition[86] utilize alternating injections of cationic and anionic precursors to grow shell on seed. For instance, Proper amount of Cd precursor and S precursor are alternatively injected into reaction mixture containing CdSe seeds to generated uniform CdS shells.[87] Another strategy is that using a less reactive sulphur precursor for shell growth. The less active precursor inhibits the homogeneous nucleation.[88] Apart from homogeneous nucleation, another profound parameter is that the mismatching of lattice between core and shell structure. It would be not easy to fabricate core-shell structure with inaccessible mismatch, thus an intermediate shell may be adopted.[89, 90]

Seed mediated growth can not only enable core-shell structure, but also symmetry-breaking structures. Au nanorods possess easy-tunable surface plasmon resonance, which is essential for optical applications[91]. However, Au nanorods are not easy to generate comparing with Au nanospherical structures, due to the requirement of symmetry breaking. To date, seed mediated growth method is the most popular method to form Au nanorod. At the beginning of the method, gold nuclei prepared by reduction of $HAuCl_4$ with phosphorus was add into $HAuCl_4$ growth solutions and growth of nanorod was initiated by the addition of H_2O_2.[92] A modified approach was broached in 2001, citrate-capped small gold nanosphere was added into a bulk $HAuCl_2$ growth solution prepared by the reduction of $HAuCl_4$ with ascorbic acid in the presence of cetyltrimethylammonium bromide (CTAB) and Ag ions, then Au nanorod could be generated.[93] The protocol was further amended in 2003, sodium citrate was replaced with CTAB.[94] Thanks to the rapidly development of high resolution characterization method, aberration-corrected phase contrast transmission electron microscopy was used to study the symmetry breaking mechanism. The symmetry breaking process occurs only for single crystalline seeds (cuboctahedral structures) at the size about 4~6 nm with the help of Ag^+. Small truncating surface lead to symmetry breaking at the intersection of {111} facets, then the deposition of new Au atoms result in rod structure.[95]

The symmetry breaking mechanism suggests that the changes of growth condition alternate the growth manner, thus novel structure can be prepared. Separating the nuclei and growth stage can also help to fabricate NPs with high index facets.[96] High index facets are usually more active for catalysts comparing with the conventional facets due to the unsaturated coordination, however on the other hand, they are more difficult to synthesis. Fabrication of metal enclosed by high index facets usually involves the introduction of metal seeds, and the kinetic control over atom deposition onto seeds. Pd concave nanocubes bounded by several [730] facets can be generated with Pd nanocubes as seeds.[97] Ag concave nanocrystals with [211] or [311], [332] facets could be obtained via cubic Ag seeds.[98] Meanwhile, the regular metal seed could serve as template for nanoframe fabrication. For example, Rh atoms can depose on the edges of Pd nanocubes, after etching the template, Rh cubic nanoframe is generated.[99] By introducing etchant, corrugated nanowires can also be generated.[100] In shsort, post growth of NPs in very different growth conditions will lead to exceptional structures.

Heterodimer NP is another symmetry breaking structure. Monodisperse metal-doped plasmonic oxide heterodimer NPs exhibit broadly tunable near-infrared localized surface plasmon resonances due to the feasible to tune the carrier concentration. M-indium-doped cadmium oxide (ICO) (M=Au, Pt, Pd, FePt, etc.) can be generated with the metal served as seeds.[101] Huge lattice stress may be one reason for the dimer structure instead of core-shell structure. A detailed study of heteroepitaxial growth of Au shell on Pt or Pt-alloy seeds found about 2 GPa on the seed by forming a core-shell structure in the early stage of the reaction.[102]

Looking beyond conserving the pristine NPs, ion exchange is an emerging method for unprecedented structural and compositional complexity. Ion exchange includes cation exchange and anion exchange, both function well in their fields. For example, the exchange of hydroxyl group with sulphur is a useful strategy to convert hydroxides to chalcogenides.[103] Sulfide NPs can undergo cation exchange as they react with Li, copper sulphide would extrude copper from crystal as they react with Li.[104] A deeper research of transformation of CdS nanowire to $Cu_{2-x}S$ nanowire provides details of cation exchange.[105] There are six stable phases found experimentally depending on reaction time and $[Cu^+]/[Cd^{2+}]$ ratio. The anionic framework is rigid and maintained during the exchange process, however, this doesn't lead to the single crystalline structure at final stage (Figure 9).

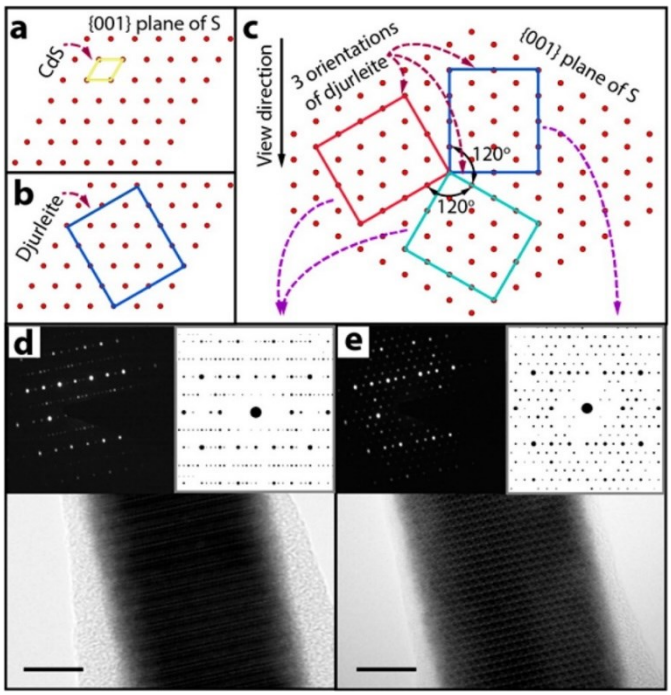

Figure 9 Relation between djurleite's unit cell and the hcp sulfur sublattice of CuS. (a, b) CdS and djurleite unit cell relative to the hcp sulfur sublattice. (c) The top direct lattice illustrations show three possible orientations of the djurleite structure relative to the hcp sulfur sublattice. (d, e) HRTEM images of two different segments taken from one NW show djurleite patterns of different orientations, with a zone axis of [012] or [01$\bar{2}$] for left, [010] for right. Scale bar, 10 nm. Inset: comparison of the simulated and experimental electron diffraction patterns. Reproduced with permission from ref. 105. Copyright 2014 ACS.

The exchange behaviours vary from bulk, nanowires and nanorods of CdS, due to the interplay between thermodynamics and kinetics. More experiments need to be done to further reveal the mystery of exchange process.

3.4 Van der Waals heterostruture

Nanoscience is a subject defined by size, the small size leads to lots of novel phenomena. The aforementioned self-assembling of clusters to form assembly has extended our research scopes of atoms. Meanwhile the atomic-thin layered materials have provoked dramatic interests for their potential in field-effect transistor.[106, 107] Looking beyond this field, alternating isolated atomic planes of different two dimensional materials can also assembled into layer by layer structure in a precisely chosen sequence, such heterostructures are often referred to "van der Waals heterostructures".[108] According to the prominent review written by A. K. Geim *et al.*[108], van der Waals heterostructures do not lack ambition. Repeating the sequence of graphene and other a few layered dielectric crystal would lead to a superficially similar structure to superconducting copper oxides, this is a worthy trying method to prepare high-T_C superconductivity. Two graphene layers separated by an ultrathin dielectric is a room-temperature excitonic superfluidity.[109, 110] However, the fabrication of van der Waals heterostructure remains challenge. Directly deposing the second layer onto pristine layer requires standard clean-room procedures and micrometre accuracy. Thus the direct chemical synthesis method may help to overcome the obstacles. In-plane $MoSe_2$–WSe_2 heterostructure could be achieved by physical vapour transport using a mixture of WSe_2 and $MoSe_2$ powder as the source.[111] In-plane WS_2/MoS_2 heterostructures could be obtained via a chemical vapour deposition, however, increasing the temperature would lead to a vertical aligned heterostructures.[112] Vertical growth of pure MoS_2 or $MoSe_2$ is also possible[113], however, they are not van der Waals heterostructures due to the lack of second compounds.

4. Conclusion

In this article, we have reviewed the post growth of particles to form new nanostructures. The inherent stabilities or interactions of NPs enables the potential morphology changes to prepare new shapes. Meanwhile, NPs or other nanomaterials are unique building units for material design and fabrications. Some detailed studies of oriented attachment or self-assembling suggest that the post growth of NPs undergoes similar kinetic process with polymerizations. These finding blurs the boundary between different chemistry and enlighten us to see things in a wider sights. The seed mediated growth provides alternating methods to optimize materials or produce morphologies that are not easy to access.

Post growth of particles contains various research interests. Deeper study of mechanism or kinetics may further extend our understanding of NPs, and further study of assembly could help to reconcile the gap between micro and macro size and the applications of various nanosized materials more feasible.

Acknowledgements
This work was supported by NSFC (21431003, 91127040, 21221062), and the State Key Project of Fundamental Research for Nanoscience and Nanotechnology (2011CB932402)

Notes and references

Department of Chemistry, Tsinghua University, Beijing, 100084, China, E-mail: wangxun@mail.tsinghua.edu.cn

1. F. Meng, S. A. Morin, A. Forticaux and S. Jin, *Acc. Chem. Res.* , 2013, **46**, 1616-1626.
2. M. Sleutel, J. Lutsko, A. E. S. Van Driessche, M. A. Durán-Olivencia and D. Maes, *Nat. Commun*, 2014, **5**, 5598.
3. A. Sauter, F. Roosen-Runge, F. Zhang, G. Lotze, R. M. J. Jacobs and F. Schreiber, *J. Am. Chem. Soc.* , 2015, **137**, 1485-1491.
4. M. Niederberger and H. Colfen, *Phys. Chem. Chem. Phys.,* 2006, **8**, 3271-3287.
5. D. Gebauer, A. Völkel and H. Cölfen, *Science*, 2008, **322**, 1819-1822.
6. E. M. Pouget, P. H. H. Bomans, J. A. C. M. Goos, P. M. Frederik, G. de With and N. A. J. M. Sommerdijk, *Science*, 2009, **323**, 1455-1458.
7. J. Rieger, M. Kellermeier and L. Nicoleau, *Angew. Chem. Int. Ed.* , 2014, **53**, 12380-12396.
8. O. D. Linnikov, *Russ. Chem. Rev.* , 2014, **83**, 343.
9. Y. Xia, Y. Xiong, B. Lim and S. E. Skrabalak, *Angew. Chem. Int. Ed.* , 2009, **48**, 60-103.
10. Z. L. Wang, *J. Phys. Chem. B*, 2000, **104**, 1153-1175.
11. Y. Wang, J. He, C. Liu, W. H. Chong and H. Chen, *Angew. Chem. Int. Ed.* , 2015, **54**, 2022-2051.
12. C. Herring, *Phys. Rev.*, 1951, **82**, 87-93.
13. H. Shu, X. Chen, X. Tao and F. Ding, *ACS Nano*, 2012, **6**, 3243-3250.
14. P. W. Voorhees, *J. Stat. Phys.* , 1985, **38**, 231-252.
15. J. A. Marqusee and J. Ross, *J. Chem. Phys.*, 1984, **80**, 536-543.
16. L. Spanhel, M. Haase, H. Weller and A. Henglein, *J. Am. Chem. Soc.* , 1987, **109**, 5649-5655.
17. A. L. Rogach, T. Franzl, T. A. Klar, J. Feldmann, N. Gaponik, V. Lesnyak, A. Shavel, A. Eychmüller, Y. P. Rakovich and J. F. Donegan, *J. Phys. Chem. C*, 2007, **111**, 14628-14637.
18. Z. A. Peng and X. Peng, *J. Am. Chem. Soc.* , 2001, **123**, 1389-1395.
19. A. Naduviledathu Raj, T. Rinkel and M. Haase, *Chem. Mater.* , 2014, **26**, 5689-5694.
20. M. N. O'Brien, M. R. Jones, K. A. Brown and C. A. Mirkin, *J. Am. Chem. Soc.* , 2014, **136**, 7603-7606.
21. T. Ma, W. Ren, Z. Liu, L. Huang, L.-P. Ma, X. Ma, Z. Zhang, L.-M. Peng and H.-M. Cheng, *ACS Nano*, 2014, **8**, 12806-12813.
22. J. Du, B. Han, Z. Liu and Y. Liu, *Cryst. Growth Des.*, 2007, **7**, 900-904.
23. Z. Chen, D. Li, W. Zhang, C. Chen, W. Li, M. Sun, Y. He and X. Fu, *Inorg. Chem.* , 2008, **47**, 9766-9772.
24. C. Zhu, G. Meng, Q. Huang, Y. Zhang, H. Tang, Y. Qian, B. Chen and X. Wang, *Chem. Eur. J.*, 2013, **19**, 9211-9217.
25. H. G. Yang and H. C. Zeng, *J. Phys. Chem. B*, 2004, **108**, 3492-3495.
26. B. Liu and H. C. Zeng, *Small*, 2005, **1**, 566-571.
27. Y. Yin, R. M. Rioux, C. K. Erdonmez, S. Hughes, G. A. Somorjai and A. P. Alivisatos, *Science*, 2004, **304**, 711-714.
28. P. Hou, P. Cui, H. Liu, J. Li and J. Yang, *Nano Res.*, 2015, **8**, 512-522.
29. Y. Wang, Y. Chen, C. Nan, L. Li, D. Wang, Q. Peng and Y. Li, *Nano Res.*, 2015, **8**, 140-155.
30. T. Vetter, M. Iggland, D. R. Ochsenbein, F. S. Hänseler and M. Mazzotti, *Cryst. Growth Des.*,, 2013, **13**, 4890-4905.
31. S.-Y. Chung, Y.-M. Kim, S.-Y. Choi and J.-G. Kim, *ACS Nano*, 2015, **9**, 327-335.

32. H. Zhang, R. L. Penn, Z. Lin and H. Colfen, *CrystEngComm*, 2014, **16**, 1407-1408.
33. R. L. Penn and J. A. Soltis, *CrystEngComm*, 2014, **16**, 1409-1418.
34. X. Xue, R. L. Penn, E. R. Leite, F. Huang and Z. Lin, *CrystEngComm*, 2014, **16**, 1419-1429.
35. L. Bahrig, S. G. Hickey and A. Eychmuller, *CrystEngComm*, 2014, **16**, 9408-9424.
36. J. H. Harding, C. L. Freeman and D. M. Duffy, *CrystEngComm*, 2014, **16**, 1430-1438.
37. L. Luo, P.-p. Wang, D. Jing and X. Wang, *CrystEngComm*, 2014, **16**, 1584-1591.
38. H. Zhang and J. F. Banfield, *CrystEngComm*, 2014, **16**, 1568-1578.
39. D. Li, M. H. Nielsen, J. R. I. Lee, C. Frandsen, J. F. Banfield and J. J. De Yoreo, *Science*, 2012, **336**, 1014-1018.
40. J. H. Yu, J. Joo, H. M. Park, S.-I. Baik, Y. W. Kim, S. C. Kim and T. Hyeon, *J. Am. Chem. Soc.* , 2005, **127**, 5662-5670.
41. K.-S. Cho, D. V. Talapin, W. Gaschler and C. B. Murray, *J. Am. Chem. Soc.* , 2005, **127**, 7140-7147.
42. L. Cademartiri, G. Guerin, K. J. M. Bishop, M. A. Winnik and G. A. Ozin, *J. Am. Chem. Soc.* , 2012, **134**, 9327-9334.
43. Y. Zhao, L. Shang, Y. Cheng and Z. Gu, *Acc. Chem. Res.* , 2014, **47**, 3632-3642.
44. K. J. M. Bishop, C. E. Wilmer, S. Soh and B. A. Grzybowski, *Small*, 2009, **5**, 1600-1630.
45. X. Ye and L. Qi, *Sci. China Chem.*, 2014, **57**, 58-69.
46. K. J. Si, D. Sikdar, Y. Chen, F. Eftekhari, Z. Xu, Y. Tang, W. Xiong, P. Guo, S. Zhang, Y. Lu, Q. Bao, W. Zhu, M. Premaratne and W. Cheng, *ACS Nano*, 2014, **8**, 11086-11093.
47. J.-M. Lehn, *Angew. Chem. Int. Ed. Engl.*, 1990, **29**, 1304-1319.
48. D. Frenkel, *Nat. Mater.* , 2015, **14**, 9-12.
49. B. de Nijs, S. Dussi, F. Smallenburg, J. D. Meeldijk, D. J. Groenendijk, L. Filion, A. Imhof, A. van Blaaderen and M. Dijkstra, *Nat. Mater.* , 2015, **14**, 56-60.
50. P. G. Bolhuis, D. Frenkel, S.-C. Mau and D. A. Huse, *Nature*, 1997, **388**, 235-236.
51. W. Song, N. Martsinovich, W. M. Heckl and M. Lackinger, *J. Am. Chem. Soc.* , 2013, **135**, 14854-14862.
52. G. Singh, H. Chan, A. Baskin, E. Gelman, N. Repnin, P. Král and R. Klajn, *Science*, 2014, **345**, 1149-1153.
53. J. Yeom, B. Yeom, H. Chan, K. W. Smith, S. Dominguez-Medina, Joong H. Bahng, G. Zhao, W.-S. Chang, S.-J. Chang, A. Chuvilin, D. Melnikau, A. L. Rogach, P. Zhang, S. Link, P. Král and N. A. Kotov, *Nat. Mater.* , 2015, **14**, 66-72.
54. B. Kahr and A. G. Shtukenberg, *Nat. Mater.* , 2015, **14**, 21-22.
55. C. Tan, X. Qi, Z. Liu, F. Zhao, H. Li, X. Huang, L. Shi, B. Zheng, X. Zhang, L. Xie, Z. Tang, W. Huang and H. Zhang, *J. Am. Chem. Soc.* , 2015, **137**, 1565-1571.
56. G. F. Zhen, J. Shu, Y. Li and C. Huang, *Sci. China Chem.*, 2013, **56**, 387-392.
57. H. Xia, G. Su and D. Wang, *Angew. Chem. Int. Ed.* , 2013, **52**, 3726-3730.
58. K. Liu, Z. Nie, N. Zhao, W. Li, M. Rubinstein and E. Kumacheva, *Science*, 2010, **329**, 197-200.
59. Y. Wang, A. D. Hollingsworth, S. K. Yang, S. Patel, D. J. Pine and M. Weck, *J. Am. Chem. Soc.* , 2013, **135**, 14064-14067.
60. L. Chen, Q. Chen, M. Wu, F. Jiang and M. Hong, *Acc. Chem. Res.* , 2014.
61. L. Cademartiri and K. J. M. Bishop, *Nat. Mater.* , 2015, **14**, 2-9.
62. S. Y. Park, A. K. R. Lytton-Jean, B. Lee, S. Weigand, G. C. Schatz and C. A. Mirkin, *Nature*, 2008, **451**, 553-556.
63. M. R. Jones, R. J. Macfarlane, B. Lee, J. Zhang, K. L. Young, A. J. Senesi and C. A. Mirkin, *Nat. Mater.* , 2010, **9**, 913-917.
64. C. Zhang, R. J. Macfarlane, K. L. Young, C. H. J. Choi, L. Hao, E. Auyeung, G. Liu, X. Zhou and C. A. Mirkin, *Nat. Mater.* , 2013, **12**, 741-746.
65. A. Kuzyk, R. Schreiber, H. Zhang, A. O. Govorov, T. Liedl and N. Liu, *Nat. Mater.* , 2014, **13**, 862-866.
66. P.-p. Wang, Q. Yu, Y. Long, S. Hu, J. Zhuang and X. Wang, *Nano Res.*, 2012, **5**, 283-291.
67. E. Auyeung, T. I. N. G. Li, A. J. Senesi, A. L. Schmucker, B. C. Pals, M. O. de la Cruz and C. A. Mirkin, *Nature*, 2014, **505**, 73-77.
68. M. A. Boles and D. V. Talapin, *J. Am. Chem. Soc.* , 2014, **136**, 5868-5871.
69. E. V. Shevchenko, D. V. Talapin, N. A. Kotov, S. O'Brien and C. B. Murray, *Nature*, 2006, **439**, 55-59.
70. R. J. Macfarlane, M. R. Jones, B. Lee, E. Auyeung and C. A. Mirkin, *Science*, 2013, **341**, 1222-1225.
71. S. Hu and X. Wang, *Sci China Chem.*, 2012, **55**, 2257-2271.
72. X. Feng, G. Li, Z. Zhang and E. Wang, *Acta Chim. Sinica*, 2013, **71**, 1575-1588.
73. X. Roy, C.-H. Lee, A. C. Crowther, C. L. Schenck, T. Besara, R. A. Lalancette, T. Siegrist, P. W. Stephens, L. E. Brus, P. Kim, M. L. Steigerwald and C. Nuckolls, *Science*, 2013, **341**, 157-160.
74. C.-H. Lee, L. Liu, C. Bejger, A. Turkiewicz, T. Goko, C. J. Arguello, B. A. Frandsen, S. C. Cheung, T. Medina, T. J. S. Munsie, R. D'Ortenzio, G. M. Luke, T. Besara, R. A. Lalancette, T. Siegrist, P. W. Stephens, A. C. Crowther, L. E. Brus, Y. Matsuo, E. Nakamura, Y. J. Uemura, P. Kim, C. Nuckolls, M. L. Steigerwald and X. Roy, *J. Am. Chem. Soc.* , 2014, **136**, 16926-16931.
75. Z. Luo and A. W. Castleman, *Acc. Chem. Res.* , 2014, **47**, 2931-2940.
76. H. Wang, L. Chen, Y. Feng and H. Chen, *Acc. Chem. Res.* , 2013, **46**, 1636-1646.
77. M. Grouchko, P. Roitman, X. Zhu, I. Popov, A. Kamyshny, H. Su and S. Magdassi, *Nat. Commun*, 2014, **5**, 2994.
78. S. Sengupta, N. Ganguli, I. Dasgupta, D. D. Sarma and S. Acharya, *Adv. Mater.* , 2011, **23**, 1998-2003.
79. W. Shi, H. Zeng, Y. Sahoo, T. Y. Ohulchanskyy, Y. Ding, Z. L. Wang, M. Swihart and P. N. Prasad, *Nano Lett.* , 2006, **6**, 875-881.
80. A. Figuerola, I. R. Franchini, A. Fiore, R. Mastria, A. Falqui, G. Bertoni, S. Bals, G. Van Tendeloo, S. Kudera, R. Cingolani and L. Manna, *Adv. Mater.* , 2009, **21**, 550-554.
81. R. Lavieville, Y. Zhang, A. Casu, A. Genovese, L. Manna, E. Di Fabrizio and R. Krahne, *ACS Nano*, 2012, **6**, 2940-2947.
82. B. Xu, H. Yang, G. Zhou and X. Wang, *Sci. China Mater.*, 2014, **57**, 34-41.
83. N. P. Dasgupta, J. Sun, C. Liu, S. Brittman, S. C. Andrews, J. Lim, H. Gao, R. Yan and P. Yang, *Adv. Mater.* , 2014, **26**, 2137-2184.
84. Y. Wu and Y. Li, *Sci. China Mater.*, 2015, **58**, 3-4.
85. A. Nag, J. Kundu and A. Hazarika, *CrystEngComm*, 2014, **16**, 9391-9407.

86. N. P. Dasgupta, X. Meng, J. W. Elam and A. B. F. Martinson, *Acc. Chem. Res.* , 2015, **48**, 341-348.
87. J. J. Li, Y. A. Wang, W. Guo, J. C. Keay, T. D. Mishima, M. B. Johnson and X. Peng, *J. Am. Chem. Soc.* , 2003, **125**, 12567-12575.
88. O. Chen, J. Zhao, V. P. Chauhan, J. Cui, C. Wong, D. K. Harris, H. Wei, H.-S. Han, D. Fukumura, R. K. Jain and M. G. Bawendi, *Nat. Mater.* , 2013, **12**, 445-451.
89. Q. Han, G. Li, D. Wang, E. He, J. Dong, W. Gao, J. Li, T. Liu, Z. Zhang and H. Zheng, *Sci. China Chem.*, 2014, **57**, 881-887.
90. Z. Wei, G Liu, X. Dong, J. Wang and W. Yu, *Acta Chim. Sinica*, 2014, **72**, 257-262.
91. X. Huang, S. Neretina and M. A. El-Sayed, *Adv. Mater.* , 2009, **21**, 4880-4910.
92. J. Wiesner and A. Wokaun, *Chem. Phys. Lett.* , 1989, **157**, 569-575.
93. N. R. Jana, L. Gearheart and C. J. Murphy, *Adv. Mater.* , 2001, **13**, 1389-1393.
94. B. Nikoobakht and M. A. El-Sayed, *Chem. Mater.* , 2003, **15**, 1957-1962.
95. M. J. Walsh, S. J. Barrow, W. Tong, A. M. Funston and J. Etheridge, *ACS Nano*, 2015, **9**, 715-724.
96. H. Zhang, M. Jin and Y. Xia, *Angew. Chem. Int. Ed.* , 2012, **51**, 7656-7673.
97. M. Jin, H. Zhang, Z. Xie and Y. Xia, *Angew. Chem. Int. Ed.* , 2011, **50**, 7850-7854.
98. X. Xia, J. Zeng, B. McDearmon, Y. Zheng, Q. Li and Y. Xia, *Angew. Chem. Int. Ed.* , 2011, **50**, 12542-12546.
99. S. Xie, N. Lu, Z. Xie, J. Wang, M. J. Kim and Y. Xia, *Angew. Chem. Int. Ed.* , 2012, **51**, 10266-10270.
100. X. Chen, A. Zhao, Q. Gao, Z. Gan and W. Tao, *Acta Chim. Sinica*, 2014, **72**, 467-472.
101. X. Ye, D. Reifsnyder Hickey, J. Fei, B. T. Diroll, T. Paik, J. Chen and C. B. Murray, *J. Am. Chem. Soc.* , 2014, **136**, 5106-5115.
102. S. G. Kwon, G. Krylova, P. J. Phillips, R. F. Klie, S. Chattopadhyay, T. Shibata, E. E. Bunel, Y. Liu, V. B. Prakapenka, B. Lee and E. V. Shevchenko, *Nat. Mater.* , 2015, **14**, 215-223.
103. W. Zhao, C. Zhang, F. Geng, S. Zhuo and B. Zhang, *ACS Nano*, 2014, **8**, 10909-10919.
104. M. T. McDowell, Z. Lu, K. J. Koski, J. H. Yu, G. Zheng and Y. Cui, *Nano Lett.* , 2015.
105. D. Zhang, A. B. Wong, Y. Yu, S. Brittman, J. Sun, A. Fu, B. Beberwyck, A. P. Alivisatos and P. Yang, *J. Am. Chem. Soc.* , 2014, **136**, 17430-17433.
106. F. Schwierz, *Nat Nano*, 2010, **5**, 487-496.
107. X. Huang and H. Zhang, *Sci. China Mater.*, 2015, **58**, 5-8.
108. A. K. Geim and I. V. Grigorieva, *Nature*, 2013, **499**, 419-425.
109. H. Min, R. Bistritzer, J.-J. Su and A. MacDonald, *Phys. Rev. B*, 2008, **78**, 121401.
110. A. Perali, D. Neilson and A. R. Hamilton, *Phys. Rev. Lett.* , 2013, **110**, 146803.
111. C. Huang, S. Wu, A. M. Sanchez, J. J. P. Peters, R. Beanland, J. S. Ross, P. Rivera, W. Yao, D. H. Cobden and X. Xu, *Nat. Mater.* , 2014, **13**, 1096-1101.
112. Y. Gong, J. Lin, X. Wang, G. Shi, S. Lei, Z. Lin, X. Zou, G. Ye, R. Vajtai, B. I. Yakobson, H. Terrones, M. Terrones, Beng K. Tay, J. Lou, S. T. Pantelides, Z. Liu, W. Zhou and P. M. Ajayan, *Nat. Mater.* , 2014, **13**, 1135-1142.
113. D. Kong, H. Wang, J. J. Cha, M. Pasta, K. J. Koski, J. Yao and Y. Cui, *Nano Lett.* , 2013, **13**, 1341-1347.

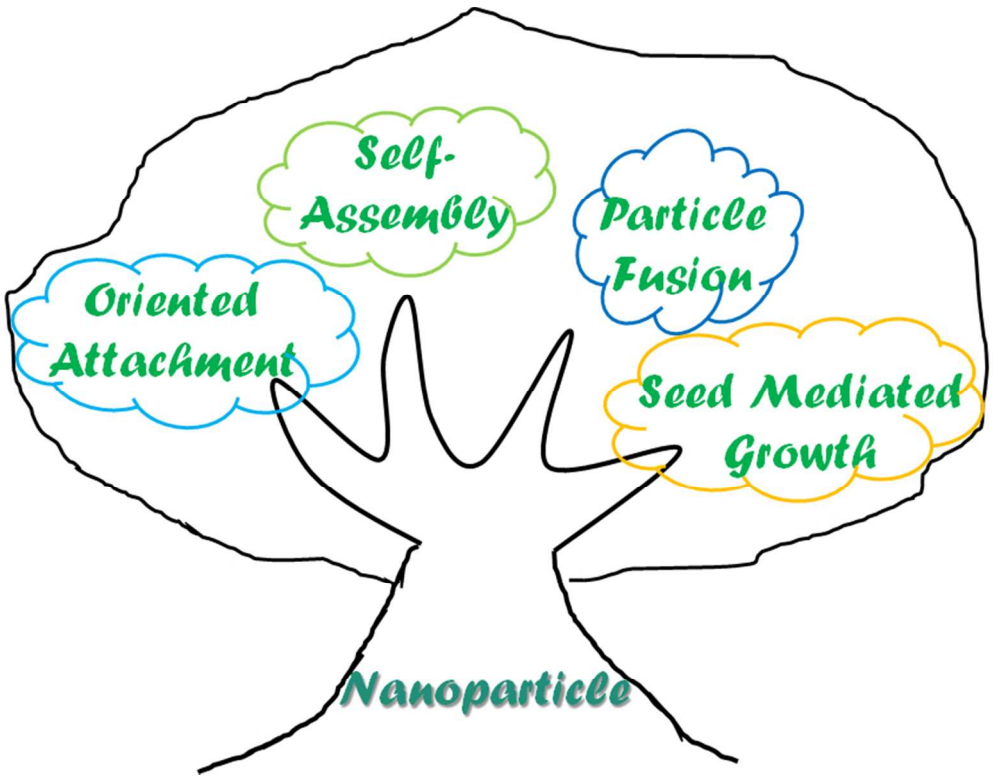

Post growth of nanoparticles enables new nanostructure formation and blurs boundary between crystals and molecules